Probing the Structure of Water Molecules at an Oil/Water Interface in the Presence of a Charged Soluble Surfactant through Isotopic Dilution Studies

D. E. Gragson[†] and G. L. Richmond*

Department of Chemistry, University of Oregon, Eugene, Oregon 97403

Received: July 25, 1997; In Final Form: October 28, 1997

We have employed vibrational sum frequency generation (VSFG) to obtain the first vibrational spectra of water molecules at an oil/water interface in the presence of a charged, soluble surfactant. By examining OH stretching modes that are highly sensitive to the local hydrogen-bonding environment, we have been able to compare the structure of interfacial water molecules with the structure of bulk water molecules determined from previous studies. From the VSFG spectra we infer that there is more extensive hydrogen bonding between neighboring water molecules at the CCl_4/water interface as compared to water molecules in the bulk aqueous phase. The presence of a charged surfactant enhances the SF response in the OH stretching spectral region in a manner similar to what we have previously observed at the air/water interface. To further probe the hydrogen bonding of water molecules at the oil/water interface, we have employed VSFG to study mixed samples of H_2O and D_2O. As the mole fraction of H_2O is decreased, the peak position of the ice-like OH stretching mode is blue-shifted by approximately 120 cm^{-1} and converges on the peak position of the uncoupled OH symmetric stretch observed in bulk ice studies. This shift in energy is discussed within the context of hydrogen bonding of the interfacial H_2O and D_2O molecules and the intermolecular uncoupling of the OH symmetric stretching vibration. Finally, we have obtained the first vibrational spectra of the OH stretching mode from uncoupled HOD molecules at the oil/water interface located at approximately 3460 cm^{-1}.

Introduction

Water structure and ordering resulting from intermolecular hydrogen bonding at various interfaces plays a substantial role in many physical processes.[1−4] Specifically, understanding the properties of interfacial water molecules is essential to the description of technological processes such as flotation, adsorption, and corrosion as well as biological processes such as micelle formation, membrane stability, and protein activity. Over the past 20 years extensive theoretical work has been conducted in an effort to better understand the structure and hydrogen bonding of interfacial water molecules at liquid/air, liquid/solid, and liquid/liquid interfaces.[3,5−7] Experimental confirmation of these theoretical studies has been slow to follow due, in part, to the limited number of techniques suitable for interfacial investigations. Within the past decade laser-based nonlinear optical techniques such as second harmonic generation (SHG) and vibrational sum frequency generation (VSFG) have been shown to be powerful tools for the study of interfaces.[8−14] In particular, the interfacial and molecular specificity of VSFG has allowed researchers to gain a better understanding of many processes at a variety of interfaces. From the work presented here we characterize the intermolecular hydrogen bonding of water molecules at an oil/water interface in the presence of a charged soluble surfactant and compare our results to the well-studied case of intermolecular hydrogen bonding in bulk liquid water.

The presence of surfactants at an oil/water interface greatly affects the surface tension of the water. In fact, this reduction of the relatively high surface tension of water by the surfactant accounts for the widespread use of surfactants in commercial products such as motor oils, lubricants, detergents, and soaps. Despite the abundant use of surfactants in these products as well as the use in many industrial processes, little is known on a molecular level about how water and surfactants interact at liquid surfaces and interfaces. This lack of information about how the presence of surfactant molecules alters the molecular orientation and intermolecular bonding of surface water molecules places severe limitations on our predictive power for designing surfactants to perform a desired task. In a recent publication we analyzed the effect of charged soluble surfactants on the structure of interfacial water molecules at the air/water interface.[10] We observed that the presence of charged surfactants at the air/water interface induced an alignment of interfacial water molecules as evidenced by a large enhancement in the sum frequency response in the OH stretching spectral region. In the work presented here we observe a similar enhancement in the VSFG spectra from an oil/water interface as the charged soluble surfactant sodium dodecyl sulfate (SDS) is added to the aqueous phase.

By examining OH stretching modes sensitive to the local hydrogen-bonding environment in H_2O, we have been able to characterize the structure of interfacial water molecules in the presence of a charged soluble surfactant. At the air/water interface we found[10,15,16] that water molecules partitioned into ice-like and water-like structures whereas in the studies presented here we find that at the oil/water interface nearly all of the water molecules are in the ice-like structure with little or no evidence for the water-like structure. This difference can be explained in terms of the effect that the nonpolar oil phase has on the interfacial water molecules, forcing them into a tetrahedral arrangement and more complete hydrogen bonding between neighboring H_2O molecules. Further characterization of the intermolecular hydrogen bonding of water molecules at an oil/water interface is investigated through isotopic dilution

[†] Department of Chemistry, Harvey Mudd College, Claremont, CA 91711.

S1089-5647(97)02444-9 CCC: $15.00
Published on Web 01/15/1998

studies. We find that as the mole fraction of H_2O is decreased, the peak position of the OH mode attributed to an ice-like structure blue-shifts by approximately 120 cm^{-1}. This shift in energy is discussed within the context of hydrogen bonding of the interfacial H_2O and D_2O molecules and an uncoupling of the OH symmetric stretching vibration. We also relate our observation to previous studies in which a blue shift in the coupled OH stretching vibration from H_2O/D_2O ice mixtures as well as super cooled liquid water was observed. Finally, we have observed for the first time the uncoupled OH stretching mode at approximately 3460 cm^{-1} from HOD molecules at the oil/water interface. We find that the spectral intensity in this mode correlates well with the calculated amount of HOD present in the H_2O/D_2O mixtures.

Background

Vibrational sum frequency generation (VSFG) is a nonlinear optical technique that has been extensively used in the study of surfaces and interfaces.[8−11,13,15] Since VSFG is a second-order nonlinear process, it is inherently surface sensitive. Further, for VSFG one combines a tunable infrared laser beam with a visible laser beam at a surface or interface. These two aspects of VSFG allow one to obtain a vibrational spectrum of molecules at an interface. The VSFG intensity is proportional to the square of the surface nonlinear susceptibility $\chi_s^{(2)}$-$(\omega_{sfg}=\omega_{vis}+\omega_{ir})$ as

$$I_{sfg} \propto |P_{sfg}|^2 \propto |\chi_{NR}^{(2)} + \sum_v |\chi_{Rv}^{(2)}| e^{i\gamma_v}|^2 I_{vis} I_{ir} \quad (1)$$

where P_{sfg} is the nonlinear polarization at ω_{sfg}, χ_{NR} and χ_{R_v} are the nonresonant and resonant parts of $\chi_s^{(2)}$, γ_v is the relative phase of the vth vibrational mode, and I_{vis} and I_{ir} are the visible and IR intensities. Since the susceptibility is in general complex, the resonant terms in the summation are associated with a relative phase γ_v which is used to account for any interference between two modes that overlap in energy. $\chi_{Rv}^{(2)}$ is also proportional to the number density of molecules, N, and the orientationally averaged molecular hyperpolarizability, β_v, as follows:

$$\chi_{Rv}^{(2)} = (N/\epsilon_0)\langle\beta_v\rangle \quad (2)$$

Thus, the square root of the measured SF intensity is proportional to the number density of molecules at the surface or interface. The molecular hyperpolarizability, β_v, is enhanced when the frequency of the IR field is resonant with a SF-active vibrational mode from a molecule at the surface or interface. This enhancement in β_v leads to an enhancement in the nonlinear susceptibility $\chi_{Rv}^{(2)}$ which can be expressed as

$$\chi_{Rv}^{(2)} \propto \frac{A_v}{\omega_v - \omega_{ir} - i\Gamma_v} \quad (3)$$

where A_v is the intensity of the vth mode and is proportional to the product of the Raman and the IR transition moments, ω_v is the resonant frequency, ω_{ir} is the tunable IR frequency, and Γ_v is the line width of the transition. Since the intensity term, A_v, is proportional to both the IR and Raman transition moments, only vibrational modes that are both IR- and Raman-active will be SF-active. Thus, molecules or vibrational modes that possess an inversion center will not be SF-active.

In general, the surface susceptibility $\chi_s^{(2)}$ is a 27-element tensor; however, it can often be reduced to several nonvanishing elements by invoking symmetry constraints. Liquid surfaces as well as monolayers on liquid surfaces are isotropic in the plane of the surface. The symmetry constraints for an in-plane isotropic surface reduces $\chi_s^{(2)}$ down to the following four independent nonzero elements

$$\chi_{zzz}^{(2)},\chi_{xxz}^{(2)} = \chi_{yyz}^{(2)},\chi_{xzx}^{(2)} = \chi_{yzy}^{(2)},\chi_{zxx}^{(2)} = \chi_{zyy}^{(2)} \quad (4)$$

where z is defined to be the direction normal to the surface. These four independent elements contribute to the VSFG under four different polarization conditions, (S,S,P) (S,P,S) (P,S,S), and (P,P,P), where the polarizations are listed in the order of decreasing frequency (sf,vis,ir). Which vibrational modes are present under a certain polarization condition depends on the polarization of the IR field and the direction of the IR and Raman transition moments. The SSP polarization condition accesses vibrational modes with transition moments that have components perpendicular to the surface plane whereas the SPS and PSS polarization conditions accesses modes that have transition moments with components parallel to the surface plane. Since the intensity under PPP polarization conditions is dependent on all of the tensor elements, vibrational modes with components both perpendicular and parallel to the surface plane will be present in these VSFG spectra. All of the vibrational modes of interfacial molecules essential to the description of the systems studied here possess transition moments with components out of the plane of the surface, requiring us to use the SSP polarization condition. However, verification of the peak assignments has been made from spectra using all of the polarization combinations.

At the oil/water interface in the presence of a charged surfactant a significant surface charge exists which produces a large electrostatic field E_0. This electrostatic field can contribute to the nonlinear polarization induced at the interface by the optical fields E_{vis} and E_{ir} through a third-order polarization term $\chi^{(3)}$ as follows:

$$P_{sfg} = \chi^{(2)}:E_{vis}E_{ir} + \chi^{(3)}:E_{vis}E_{ir}E_0 \quad (5)$$

The second term in eq 5 is the third-order polarization term, $P_{sfg}^{(3)}$, and contains the electrostatic field dependence of the nonlinear polarization induced at the interface. Both $\chi^{(3)}$ and $\chi^{(2)}$ have resonant and nonresonant portions as described above, and in fact the overall SF response can be represented by an effective surface susceptibility that is a combination of $\chi^{(3)}$ and $\chi^{(2)}$. The third-order contribution to the nonlinear polarization results from several factors, namely, the electronic nonlinear polarizability, $\alpha^{(3)}$, the alignment of the interfacial water molecules by the electrostatic field E_0, and the magnitude of the electrostatic field E_0. In the absence of an electrostatic field the interfacial water molecules are randomly oriented after a few water layers, and thus only these first few layers contribute to the nonlinear polarization. The presence of a large electrostatic field aligns the interfacial water molecules beyond the first few water layers and thus removes the centrosymmetry over this region, allowing more water molecules to contribute to the nonlinear polarization. The depth of the asymmetric region is on the order of the Debye length or 3 nm at an ionic strength of 10 mM and 10 nm at an ionic strength of 1.0 mM, corresponding to approximately 10−30 water layers. Previous studies have shown[10,12,15,17,18] that this alignment of the interfacial water molecules is manifested in the VSFG spectra as a large enhancement in the SF response in the OH stretching spectral region.

Experimental Section

The laser system employed for the vibrational SFG studies has been described in detail elsewhere.[19,20] Briefly it consists of a titanium:sapphire regenerative amplifier that pumps a two-stage optical parametric amplifier seeded with a small portion of white light continuum. The system produces IR pulses tunable from 2.4 to 4.0 μm at a repetition rate of 1 kHz. The energy of the pulses over this range is approximately 10 μJ with a bandwidth of 18 cm^{-1} and a pulse duration of 1.9 ps. The IR pulses are combined at the interface with approximately 150 μJ of 800 nm light from the Ti:sapphire regenerative amplifier. The beam diameter of the tunable IR and 800 nm laser beams are approximately 300 μm and 4 mm, respectively. All spectra presented were obtained under S_{sfg}, S_{vis}, P_{ir} polarization conditions which picks out the vibrational modes with components of the transition dipole moment perpendicular to the plane of the interface. Spectra from the CCl_4/water interface were obtained in an internal reflection geometry with the 800 nm and tunable IR beams coincident on the interface from the CCl_4 side at the critical angle for each wavelength (66.5° and 73.2°, respectively). Previous studies have shown[8,13] that operating in a total internal reflection geometry produces an enhancement of several orders of magnitude in the generated nonlinear polarization. The generated sum frequency light is detected in reflection with a PMT after filtering. Individual spectra were collected with gated electronics and a computer while the IR frequency was scanned from 2750 to 3700 cm^{-1}. Our laser system limits our ability to obtain reliable spectra in the 3600−4000 cm^{-1} region;[20] thus, we limit our discussion to the 2750−3600 cm^{-1} spectral region. Each scan was obtained with an increment of 4 cm^{-1} and an average of 300 laser shots per increment, and each spectrum presented is an average of at least two scans.

Both 18 MΩ water from a Nanopure filtration system and HPLC grade water from Mallinckrodt were used with no detectable difference in the VSFG spectra. D_2O (99.9 atom %) from Aldrich was thoroughly mixed with CCl_4 and decanted off to remove any organic contaminants. HPLC grade carbon tetrachloride (99.9+%) from Sigma-Aldrich was used as received. Both 99% sodium dodecyl sulfate from Sigma-Aldrich and 98 atom % d_{25}-sodium dodecyl sulfate from Cambridge isotope laboratories were used as received. SDS (1.00 mM) in H_2O/D_2O solutions were made by making additions of 1.00 mM SDS in H_2O to 1.00 mM SDS in D_2O solutions and additions of 1.00 mM SDS in D_2O to 1.00 mM SDS in H_2O solutions. The mole fractions of H_2O, D_2O, and HOD were calculated by assuming complete isotopic exchange and the equilibrium $H_2O + D_2O = 2HOD$ with an equilibrium constant $K = 4$.[21,22] Absorption of the tunable IR beam in the OH stretching region by the CCl_4 was determined to be negligible with FTIR and by monitoring the IR energy after the beam had traversed a 1 cm path length of CCl_4. All glassware and experimental apparatus that came into contact with the aqueous or organic phases were soaked in concentrated sulfuric acid containing No-Chromix for at least 3 h and then were thoroughly rinsed with 18 MΩ water.

Results

A. Sodium Dodecyl Sulfate at the Oil/Water Interface. Figure 1 shows the VSFG spectra from the CCl_4/H_2O interface in the OH stretching spectral region with varying bulk concentrations of the charged soluble surfactant SDS present in the aqueous phase. We used completely deuterated SDS to remove the interferences between the CH and OH stretching modes found in earlier studies,[10,15] allowing us to obtain more accurate fitted data for the water modes. The solid lines in Figure 1 are a least-squares fit to the data using eqs 1 and 3 from which we are able to extract peak intensities, positions, bandwidths, and integrated areas. Table 1 lists the OH stretching modes typically observed in IR and Raman spectroscopic studies of bulk water along with the structural characteristics of each mode.

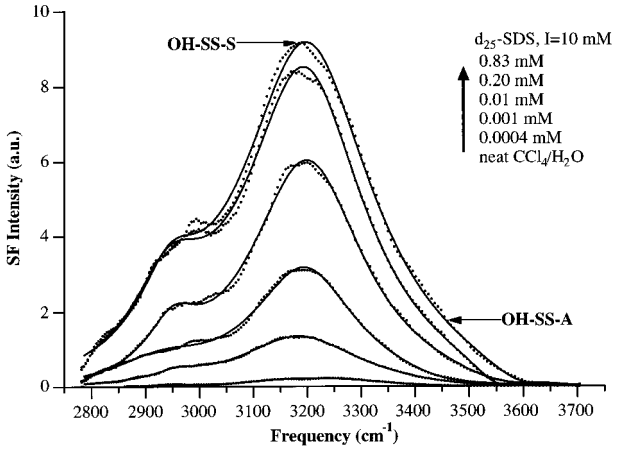

Figure 1. VSFG spectra from the CCl_4/H_2O interface with varying bulk concentrations of d_{25}-SDS under S-sf, S-vis, P-ir polarization conditions. Solid lines are a fit to the data using eqs 1 and 3.

As was mentioned earlier, the presence of a surface charge resulting from the adsorption of charged surfactant to the interface induces an electrostatic field across the interfacial region. This electrostatic field can be as large as 10^8 V/m and can induce an alignment of the dipoles of the interfacial water molecules. This alignment is manifested in the VSFG spectrum as an enhancement in the SF signal in the OH stretching spectral region. Inspection of the spectra in Figure 1 shows that there is a large enhancement in the SF signal as the bulk surfactant concentration is increased. This increase with increasing bulk concentration is a result of the fact that the interfacial concentration, and thus the surface charge density and magnitude of the electrostatic field, is a function of the bulk concentration. We find that this enhancement reaches a maximum value slightly below a bulk concentration of 1.0 mM while surface tension measurements show that the maximum surface coverage occurs around 2−3 mM. Further, we observe an enhancement in the SF response at sub-micromolar bulk concentrations that correspond to surface concentrations several orders of magnitude below the maximum surface concentration. The ability to detect a very low surface concentration of SDS illustrates the high sensitivity of this experimental technique.

In a recent publication[16] we showed that at the neat oil/water interface the prevailing structure of the water molecules is a tetrahedral arrangement much like the structure of ice, while at the neat air/water interface we observed an equal distribution between an ice-like and a less ordered water-like arrangement. Inspection of the spectra in Figure 1 shows that as charged surfactant is added to the aqueous phase, the dominant spectral feature remains the OH−SS−S (ice-like) mode whereas there is little or no evidence for intensity from the OH−SS−A (water-like) mode. The shoulder in the 2900−3050 cm^{-1} region arises from a small amount of contaminant, CH stretches, present at the neat interface riding on the large OH peak and possibly the OH stretch from water molecules strongly hydrogen bonded to the sulfate headgroup. From the dominance of the OH−SS−S mode we infer that the prevailing structure of the interfacial water molecules in the presence of a charged surfactant is a tetrahedral arrangement much like the structure of ice. This

TABLE 1: Peak Assignments and Bandwidths for OH Stretching Modes of H_2O and HOD

OH mode label	structural designation	freq (cm^{-1})	fwhm (cm^{-1})	ref
OH−SS−S, H_2O	ice-like, high H-bond order	3200−3250	310	21, 27
OH−SS-A, H_2O	water-like, low H-bond order	3400−3450	260	21, 27
uncoupled OH−S, HOD	inter- and intramolecularly uncoupled OH	3300−3500	260	21, 22
free-OH	non-hydrogen-bonded	3680	70	18

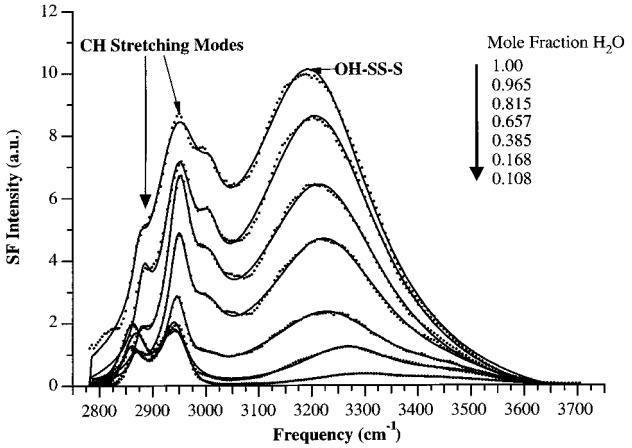

Figure 2. VSFG spectra from the CCl_4/H_2O interface with 1.0 mM SDS in the aqueous phase as a function of mole fraction of H_2O under S-sf, S-vis, P-ir polarization conditions.

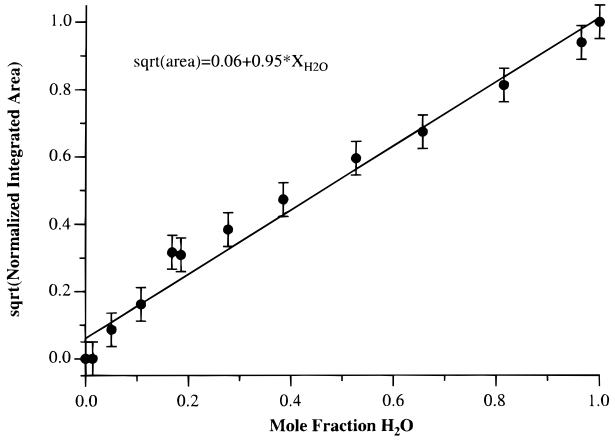

Figure 3. Plot of the square root of the normalized integrated area of the OH−SS−S mode, determined from fits to eqs 1 and 3, as a function of the mole fraction of H_2O. Solid line is a linear fit to the data.

observation is in striking contrast to the IR and Raman spectra from bulk water at room temperature[23] for which there is approximately equal distribution between each mode. As will be discussed below, this difference implies that the hydrogen bonding between neighboring water molecules is more complete at the oil/water interface as compared to water molecules in the bulk aqueous phase.

B. Isotopic Dilution. Figure 2 shows the VSFG spectra for various mixtures of H_2O and D_2O ranging from a H_2O mole fraction of 1.00 to 0.1 in the presence of the charged soluble surfactant SDS held constant at a bulk concentration and ionic strength of 1.00 mM. The mole fraction of H_2O was calculated assuming complete isotopic exchange and the equilibrium $H_2O + D_2O = 2HOD$ with $K = 4$. For Figure 2 we have used hydrogenated SDS, and the CH stretching modes are indicated on the spectra. These modes include the CH_2 symmetric stretch (2850 cm^{-1}), the CH_3 symmetric stretch (2875 cm^{-1}), the CH_3 Fermi resonance (2935 cm^{-1}), and the CH_2 asymmetric stretch (2937 cm^{-1}). The 20 cm^{-1} bandwidth of the IR laser beam makes resolution of these peaks difficult, and thus further discussion of the CH modes is not warranted here. We have performed other studies[8,10,13,15] that specifically address the spectroscopy of the surfactant at the CCl_4/water interface without the complication of limited resolution. The shoulder in the spectra located at approximately 3000 cm^{-1} could be due to the OH stretch from water molecules that are hydrogen-bonded to the charged sulfate headgroup with the large red shift presumably a result of the strong hydrogen bond. We have also observed a shoulder in this region from surfactants with sulfonate headgroups.[24] We observe intensity in this spectral region from the deuterated SDS studies as well, but strangely we have not observed the shoulder in air/water studies with surfactants with either headgroup. The solid lines in Figure 2 are a least-squares fit to the data using eqs 1 and 3 from which we are able to extract peak intensities, positions, bandwidths, and integrated areas. We fit each spectrum to five peaks: two due to CH stretching modes, two due to OH stretching modes, and the last being the aforementioned mode at approximately 3000 cm^{-1}.

Inspection of Figure 2 shows that the OH−SS−S mode dominates the VSFG spectrum from the oil/water interface while there is little or no evidence of the OH−SS−A mode. The OH−SS−S mode is present in both the VSFG spectra from the air/water interface and the IR and Raman spectra from bulk water, thus indicating a preference for an ice-like structure at the oil/water interface. As the mole fraction of H_2O is decreased by adding D_2O, we observe a decrease in the intensity of the OH−SS−S mode resulting from fewer H_2O molecules contributing to the SF signal. For linear spectroscopies the integrated area of a particular peak is proportional to the number of oscillators contributing to that peak. For the case of VSFG the SF response is proportional to the square of the number of oscillators contributing to the signal; thus, within the confines of eqs 1 and 3 the number of interfacial H_2O molecules contributing to the OH−SS−S mode is proportional to the square root of the integrated area for the OH−SS−S peak. Figure 3 shows a plot of the square root of the integrated area versus the mole fraction of H_2O where the square root of the integrated area has been normalized to one for a H_2O mole fraction of unity. The solid line in Figure 3 is a linear fit to the data with the functionality expressed on the graph. The linear dependence of the square root of the integrated area on the mole fraction of H_2O shows that the square root of the area is a good measure of the relative number of oscillators contributing to the OH−SS−S peak in the VSFG spectra.

C. Interfacial HOD Molecules. Figure 4 shows the VSFG spectra from the lowest mole fraction H_2O solutions studied with the SF intensity axis expanded so the OH features can be more easily discerned. From inspection of the 0.108 mole fraction H_2O solution spectra we observe a small shoulder at approximately 3460 cm^{-1} on the high-frequency side of the blue-shifted OH−SS−S peak from interfacial H_2O molecules. We attribute this peak at approximately 3460 cm^{-1} to the uncoupled OH stretch (OH−S) from interfacial HOD molecules produced by isotopic exchange between H_2O and D_2O. The VSFG spectrum from the 0.05 mole fraction H_2O solution shows that this peak actually dominates the OH stretching spectral region. This observation is a result of the very small concentra-

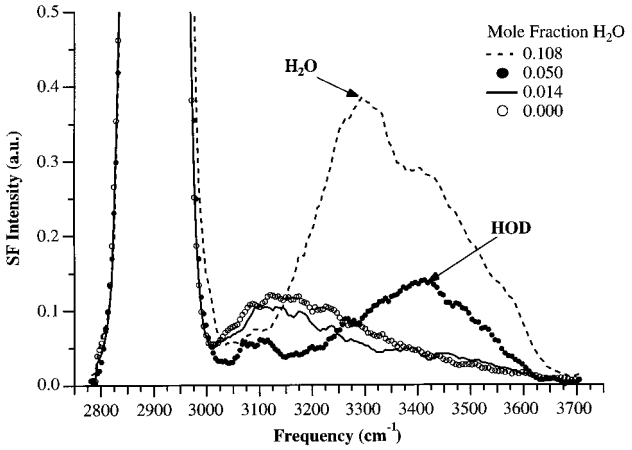

Figure 4. VSFG spectra from the CCl_4/H_2O interface with 1.0 mM SDS in the aqueous phase for low mole fractions of H_2O under S-sf, S-vis, P-ir polarization conditions.

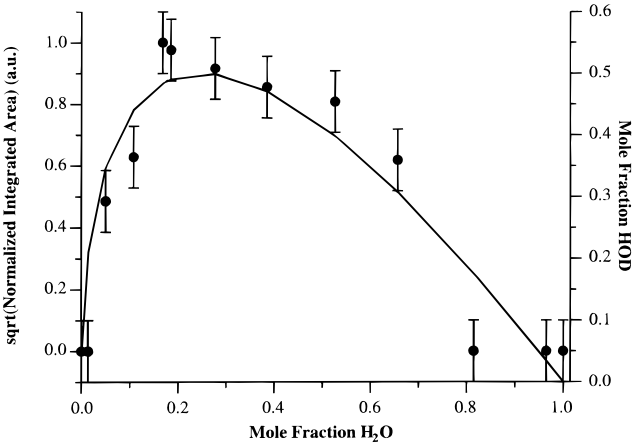

Figure 5. Plot of the square root of the normalized integrated area of the OH−SS mode from HOD molecules, determined from fits to eqs 1 and 3, as a function of the mole fraction of H_2O. Solid line is a plot of the mole fraction of HOD as a function of the mole fraction of H_2O calculated using the equilibrium $H_2O + D_2O = 2HOD$ and $K = 4$.[21,22]

tion of H_2O and the much larger (0.35 mole fraction) HOD concentration. The absolute intensity from the OH stretch of HOD is much weaker than the OH stretch of H_2O. This decrease in intensity is a result of diminished hydrogen bonding and uncoupling of the OH stretching vibration from interfacial HOD molecules.

We have fit the VSFG spectra for all the mole fraction solutions studied using two OH modes, the OH−SS−S from H_2O and the OH−S from HOD, according to eqs 1 and 3. Using the fitted peaks, we have calculated the integrated area of the OH−S mode from interfacial HOD as a function of H_2O mole fraction. As mentioned earlier, the square root of the area of a peak in the VSFG spectrum is a good measure of the number of oscillators contributing to the SF signal; thus, in Figure 5 we plot the normalized square root of the peak area of the OH−S mode from interfacial HOD molecules as a function of the mole fraction of H_2O. On the same figure we plot the mole fraction of HOD as a function of the mole fraction of H_2O calculated assuming complete isotopic exchange and the equilibrium $H_2O + D_2O = 2HOD$ with $K = 4$.[21,22] The agreement between the square root of the area of the peak at 3460 cm^{-1} and the mole fraction of HOD provides further evidence that the OH−S from HOD molecules is responsible for this peak. This work represents the first observation of the OH stretch from uncoupled HOD molecules at an oil/water interface in the presence of a charged soluble surfactant.

Discussion

A. Effect of a Charged Surfactant on the Interfacial Water Structure. The structural properties of bulk water have been previously characterized in numerous studies through inspection of the OH stretching modes in Raman and IR spectra. Table 1 lists the peak positions of the OH stretching modes for H_2O and HOD along with the bandwidths of each transition as observed from Raman and IR measurements. From the presence of each of these modes, researchers have been able to infer the structure of water molecules in a variety of systems.[11,15,23,25−28] The OH−SS−S mode located between 3200 and 3250 cm^{-1} is attributed to the coupled symmetric stretch from water molecules that have complete tetrahedral coordination with two strong hydrogen bonds much like the structure of ice. The mode located between 3400 and 3450 cm^{-1} is attributed to the coupled symmetric stretch from water molecules that have incomplete tetrahedral coordination with one strong and one weaker hydrogen bond. Raman and IR spectroscopic studies have shown that the peak at 3200 cm^{-1} dominates the spectra of bulk liquid water at low temperatures whereas the peak at 3450 cm^{-1} dominates the spectra at elevated temperatures.[23,27] The temperature dependence of the spectral features has led researchers to characterize these two peaks as being indicative of "ice-like" (OH−SS−S) and "water-like" (OH−SS−A) structures with the ice-like mode corresponding to a higher degree of hydrogen bond ordering and the water-like mode corresponding to a lower degree of hydrogen bond ordering.

A third OH mode observed in previous bulk and surface water studies is located at approximately 3680 cm^{-1} and is attributed to the free OH stretch from water molecules that have hydrogen atoms not participating in hydrogen bonding. As was mentioned earlier, the ability to obtain spectra in the 3600−4000 cm^{-1} region is limited by the laser system; thus, we typically do not observe this peak in the VSFG spectra. The red shift of the peak position of the OH stretching modes with increased intermolecular coupling caused by increased hydrogen bonding as seen in the three aforementioned modes has been thoroughly examined.[27,29,30,31] The shift occurs because hydrogen bonding actually "steals" bond strength from the OH bond, and thus stronger hydrogen bonds result in weaker OH covalent bonds and vibrational modes at lower energy. A comparison of the peak positions with the degree of hydrogen bonding illustrates the well-known trend that the peak position of the OH stretching mode is red shifted with increasing hydrogen bonding. Accompanying the red-shift of the peak frequency with increased hydrogen bonding is a large increase in the bandwidth of the OH stretch. This increase in the bandwidth results from dynamic dipole−dipole coupling between neighboring water molecules which produces a distribution of low- and high-frequency stretching modes.[27,29,30,31] The nature of this distribution also has an effect on the position of the peak frequency of the OH stretching mode. Deconvolution of these two effects, hydrogen bonding and intermolecular coupling, on the energetics of the OH stretching peaks in the vibrational spectra is difficult and generally requires the study of HOD in H_2O or D_2O which eliminates the intermolecular coupling effect. However, the extent of hydrogen bonding can be inferred through a comparison of the relative amount of each coupled mode, OH−SS−S and OH−SS−A, present in the vibrational spectra. This comparison is possible since the ice-like (OH−SS−S) peak is indicative of more complete or more extensive hydrogen bonding than the water-like (OH−SS−A) peak.

Our observation that at the oil/water interface the OH−SS−S mode dominates the OH stretching spectral region provides direct evidence that there is more extensive hydrogen bonding between neighboring interfacial water molecules when compared to bulk water molecules. This difference is a result of the effect that the nonpolar CCl_4 molecules have on the water molecules in the interfacial region. This effect can be explained in terms of the ability of water to solvate a nonpolar molecule such as CCl_4 and the corresponding decrease in entropy associated with the solvation of nonpolar molecules.[1,4,29,32] This decrease in the entropy of the system overrides the enthalpy of solvation and causes the solvation of nonpolar molecules in water to be energetically unfavorable. The decrease in entropy is thought to result from water molecules rearranging into a tetrahedral structure in order to maximize hydrogen bonding in the presence of a nonpolar solute.[1,4,29,32] Our observation that the VSFG spectrum is dominated by the ice-like peak at the CCl_4/water interface is a direct manifestation of the structure-inducing influence of CCl_4 molecules on the interfacial water molecules. This observation is also consistent with previous calculations of hydrogen bonding at an oil/water interface which suggest that there is an increase in the strength of the hydrogen bonding among the water molecules near a hydrophobic surface.[33] As was mentioned earlier, we are probing specifically the asymmetric interfacial region which for the studies discussed here, ionic strength of 10 mM, corresponds to at most 10 water layers. In the bulk aqueous phase the water molecules are not influenced by the presence of a nonpolar molecule, and thus the water-like peak accompanies the ice-like peak. The similarity of the water structure at the oil/water interface both in the presence and in the absence of a charged soluble surfactant further allows us to infer that the presence of the surfactant and counterions in the aqueous phase does not disrupt the bond ordering of the interfacial water molecules.

B. Spectroscopy from Varying Mixtures of H_2O and D_2O. Numerous IR and Raman studies of H_2O/D_2O mixtures have been conducted in the past to gain a better understanding of the structure of water in both bulk liquid water and bulk ice.[21−23,31,34−41] The reasoning behind these studies is that as D_2O (H_2O) is added to H_2O (D_2O), the intermolecular coupling between the OH (OD) oscillators decreases as a result of the difference in energy of the OH and OD stretches and the difference in hydrogen bonding between H_2O and D_2O. The intermolecular decoupling as D_2O (H_2O) is added to H_2O (D_2O) manifests itself in the IR and Raman spectra as a blue shift in the spectral position of the OH (OD) stretching vibrations. This blue shift occurs as the mole fraction of H_2O (D_2O) is decreased and is a result of the decreased intermolecular coupling of the OH stretches between neighboring H_2O molecules. Experiments conducted on both cubic and amorphous ice have shown[34,39] a blue shift in the OH−SS−S peak of approximately 100−120 cm^{-1} as the mole fraction of H_2O varies from 1.00 to 0.01 with the peak position of the OH stretch converging on the uncoupled mode at 3225 cm^{-1}. In an effort to further characterize the structure of water molecules at the oil/water interface in the presence of charged surfactants, we have conducted VSFG experiments on mixtures of H_2O and D_2O to probe the hydrogen bonding of interfacial water molecules.

Close inspection of the spectra in Figure 2 shows that we are sensitive to the expected blue shift of the OH−SS−S peak position with decreasing H_2O mole fraction. The peak position goes from a value of 3200 cm^{-1} at a mole fraction of 1.00 to a value of 3320 cm^{-1} at a mole fraction of 0.05. The blue shift in the peak frequency of the OH−SS−S with decreasing H_2O mole fraction is a result of the intermolecular decoupling of the OH oscillators by the addition of OD oscillators as previously mentioned. The magnitude of the blue shift that we observe for H_2O molecules at the oil/water interface in the presence of SDS is approximately the same, 120 cm^{-1}, as has been observed for both bulk amorphous ice and cubic ice[34,39] as well as supercooled water at −5 °C.[31] From this similarity we infer that the water molecules at the oil/water interface are indeed very much in an ice-like arrangement with a high degree of hydrogen bond order and a tetrahedral structure. Figure 6 shows the peak frequency of the OH−SS−S stretch obtained from the fits to the spectral data using eqs 1 and 3 plotted as a function of the mole fraction of H_2O. From Figure 6 we see that the peak frequency of the OH−SS−S mode blue-shifts in nominally a linear fashion with decreasing H_2O mole fraction over the range from 1.0 to 0.2. Beyond a mole fraction of 0.2 the slope of the frequency shift with decreased H_2O becomes significantly steeper. This observation is most likely due to the increased HOD component present at the interface interfering with the fitting of the spectra.

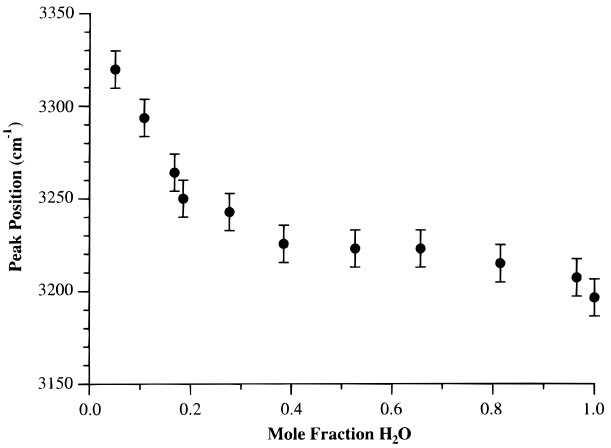

Figure 6. Plot of the peak position of the OH−SS−S mode as a function of the mole fraction of H_2O from the data fitted according to eqs 1 and 3.

C. Uncoupled Interfacial HOD Molecules. Along with the uncoupling of the OH stretching modes that occurs as D_2O is added to H_2O, one also expects that HOD will be produced. Numerous IR and Raman spectroscopic studies have been performed on isotopic solutions of HOD in H_2O and D_2O in bulk liquid water and ice forms.[22,23,31,34,37,38,40] The reason for these studies is the simplified spectrum of HOD as compared to that of H_2O or D_2O.[22] This simplification is a result of two main factors: first, the OH (OD) stretching mode of HOD in D_2O (H_2O) is intermolecularly uncoupled due to the dilution of the strong interaction between neighboring oscillators with bending and stretching modes overlapping in energy, and second, the OH and OD stretching modes of HOD are intramolecularly uncoupled due to the isotopic mass difference. The fact that HOD is both intermolecularly and intramolecularly uncoupled simplifies the interpretation of the vibrational spectrum. A result of this simplification is that the vibrational spectrum of HOD in both H_2O and D_2O can been used by researchers to elucidate structural characteristics of bulk liquid water and solid ice.

Researchers using polarized Raman spectroscopy have suggested a two-species model for the hydrogen-bonded HOD molecules in bulk water solutions.[23] The first species is composed of water molecules with two equivalent strong hydrogen bonds while the second is composed of water molecules with one weak and one strong hydrogen bond. Using

this scheme, one predicts that there are two OH and two OD stretching modes within each case: one corresponding to stronger hydrogen bonding and one corresponding to weaker hydrogen bonding. The OH stretch from the more strongly hydrogen bonded HOD in D_2O has been shown[21,23,35,38] to occur between 3300 and 3500 cm^{-1} and is very temperature sensitive, shifting to higher frequencies with an increase in temperature. The peak position of the more strongly hydrogen-bonded OH (OD) stretching mode in the liquid state varies from 3435 to 3489 cm^{-1} (2520 to 2568 cm^{-1}) as the temperature varies from 10 to 90 °C.[23] In contrast, the peak position of the more weakly hydrogen-bonded OH (OD) from HOD in D_2O (H_2O) has been shown to be relatively temperature independent, remaining relatively fixed at approximately 3600 cm^{-1} (2650 cm^{-1}). Our observation that the OH stretch from interfacial HOD molecules at room temperature is located at approximately 3460 cm^{-1} seems to be in fair agreement with the position of the more strongly hydrogen-bonded OH stretch. Assuming a linear dependence of the OH stretch peak position on the temperature, one finds that the peak position blue-shifts approximately 6.8 cm^{-1} for every 10 °C over the range 10−90 °C. Using this functionality and our peak position at 3460 cm^{-1}, we arrive at a value of approximately 47 °C for our interfacial temperature. The fact that the interfacial temperature derived by the method introduced above is higher than the room temperature at which the experiments were conducted is possibly the result of two main factors. First, the intensity of the laser beams could produce local heating of the interfacial water molecules and thus be the source of the higher interfacial temperature. However, in related temperature-dependent experiments at oil/water and air/water interfaces,[24] we find negligible evidence for local heating by the laser beams. The other possibility is that both of the OH stretching modes from the interfacial HOD molecules, the more weakly hydrogen-bonded and the more strongly hydrogen-bonded modes, are present in the broad peak at 3460 cm^{-1}, and the incorporation of the more weakly hydrogen-bonded mode at 3600 cm^{-1} into the fits might red-shift the more strongly hydrogen-bonded peak. Our attempts to include the higher energy mode produced fits that were in poor agreement with the spectral data, and thus this also seems to be an unlikely explanation. Additional studies involving the variation of beam intensities are currently in progress to further explore the possibility of local heating.

Conclusion

We have employed vibrational sum frequency generation to study the structure of water molecules at the oil/water interface in the presence of a charged soluble surfactant. We have obtained for the first time the vibrational spectrum of water molecules at an oil/water interface in the presence of a charged soluble surfactant. Through a comparison of OH stretching modes sensitive to the local environment of water molecules we infer that the water molecules at the CCl_4/water interface both in the presence and absence of charged soluble surfactants are predominantly in a tetrahedral arrangement much like the structure of ice. As a charged soluble surfactant is added to the aqueous phase we observe a large enhancement in the SF signal in the OH stretching spectral region similar to what we have previously observed from air/water studies. We observe this enhancement at surface concentrations several orders of magnitude below maximum surface coverage which illustrates the high degree of sensitivity possible with the technique. We attribute this enhancement to an alignment of the interfacial water molecules resulting from the large electrostatic field produced by the surface charge from the surfactant molecules adsorbed to the interface. This alignment is present further into the bulk phase than for the case of the neat oil/water interface as evidenced by the much larger SF response in the OH stretching spectral region.

We have further characterized the hydrogen bonding of water molecules at the CCl_4/water interface by obtaining the VSFG spectra from various mixtures of H_2O with D_2O. We observe that the square root of the area of the OH−SS−S peak in the VSFG spectra linearly depends on the mole fraction of H_2O confirming our use of the square root of the area as a relative measure of the number of oscillators interacting with the optical fields. We also observe a blue-shift of approximately 120 cm^{-1} in the OH−SS−S peak with decreasing H_2O mole fraction which we attribute to intermolecular uncoupling of the OH oscillators. The similarity in the magnitude of this frequency shift with the frequency shift observed from bulk amorphous and cubic ice further confirms our conclusion that the interfacial water molecules are in an ice-like arrangement. Finally, we have observed for the first time the OH stretching mode located at approximately 3460 cm^{-1} from HOD molecules at an oil/water interface in the presence of a charged soluble surfactant. This mode has been shown to be essential in the full characterization of the structure of bulk water in both liquid and solid phases from IR and Raman spectroscopic studies. Our future endeavors will include exploiting this mode to probe the interfacial hydrogen bonding environment as a function of temperature and the presence of structure making and breaking ions as well as to probe the dependence on the interfacial potential.

Acknowledgment. The authors thankfully acknowledge the Office of Naval Research and the National Science Foundation (CHE-9416856) and the Petroleum Research Fund of the American Chemical Society for support of this work.

References and Notes

(1) Jones, M. N.; Chapman, D. *Micelles, Monolayers, and Biomembranes*; Wiley-Liss: New York, 1995.
(2) Gawrisch, K.; Ruston, D.; Zimmerberg, J.; Parsegian, V. A.; Rand, R. P. *Biophys. J.* **1992**, *61*, 1213−23.
(3) Benjamin, I. *Chem. Rev. (Washington, D.C.)* **1996**, *96*, 1449−1475.
(4) Tanford, C. *The Hydrophobic Effect*; Wiley-Interscience: New York, 1973.
(5) Carpenter, I. L.; Hehre, W. J. *J. Phys. Chem.* **1990**, *94*, 531.
(6) Lee, C. Y.; McCammon, J. A.; Rossky, P. J. *J. Chem. Phys.* **1984**, *80*, 4448−55.
(7) Schweighofer, K. J.; Xia, X.; Berkowitz, M. L. *Langmuir* **1996**, *12*, 3747−3752.
(8) Conboy, J. C.; Messmer, M. C.; Richmond, G. L. *J. Phys. Chem.* **1996**, *100*, 7617−7622.
(9) Bell, G. R.; Bain, C. D.; Ward, R. N. *J. Chem. Soc., Faraday Trans.* **1996**, *92*, 515−523.
(10) Gragson, D. E.; McCarty, B. M.; Richmond, G. L. *J. Phys. Chem.* **1996**, *100*, 14272−14275.
(11) Du, Q.; Freysz, E.; Shen, Y. R. *Science (Washington, D. C.)* **1994**, *264*, 826−8.
(12) Zhao, X.; Ong, S.; Eisenthal, K. B. *Chem. Phys. Lett.* **1993**, *202*, 513−520.
(13) Messmer, M. C.; Conboy, J. C.; Richmond, G. L. *J. Am. Chem. Soc.* **1995**, *117*, 8039−40.
(14) He, G.; Elking, M. D.; Xu, Z. *Chem. Phys. Lett.* **1996**, *245*, 184−90.
(15) Gragson, D. E.; McCarty, B. M.; Richmond, G. L. *J. Am. Chem. Soc.* **1997**, *119*, 6144−52.
(16) Gragson, D. E.; Richmond, G. L. *Langmuir*, in press.
(17) Ong, S.; Zhao, X.; Eisenthal, K. B. *Chem. Phys. Lett.* **1992**, *191*, 327−335.
(18) Du, Q.; Freysz, E.; Shen, Y. R. *Phys. Rev. Lett.* **1994**, *72*, 238−41.
(19) Gragson, D. E.; Alavi, D. S.; Richmond, G. L. *Opt. Lett.* **1995**, *20*, 1991−1993.

(20) Gragson, D. E.; McCarty, B. M.; Richmond, G. L.; Alavi, D. S. *J. Opt. Soc. Am. B* **1996**, *13*, 2075−2083.
(21) Scherer, J. R.; Snyder, R. G. *J. Chem. Phys.* **1977**, *67*, 4794−4811.
(22) Wiafe-Akenten, J.; Bansil, R. *J. Chem. Phys.* **1983**, *78*, 7132−37.
(23) Scherer, J. R.; Go, M. K.; Kint, S. *J. Phys. Chem.* **1974**, *78*, 1304−13.
(24) Gragson, D. E.; Richmond, G. L. To be Published.
(25) D'Angelo, M.; Martini, G.; Onori, G.; Ristori, S.; Santucci, A. *J. Phys. Chem.* **1995**, *99*, 1120−23.
(26) Yalamanchili, M. R.; Atia, A. A.; Miller, J. D. *Langmuir* **1996**, *12*, 4176−4184.
(27) Rice, S. A. Topics in Current Chemistry. In *Topics in Current Chemistry*; Springer-Verlag: New York, 1975; Vol. 60, pp 109−201.
(28) *Water: A Comprehensive Treatise*; Walrafen, G. E., Ed.; Plenum Press: New York, 1972; Vol. 1, pp 151−254.
(29) Eisenberg, D.; Kauzmann, W. *The Structure and Properties of Water*; Oxford University Press: New York, 1969.
(30) Whalley, E. *Can. J. Chem.* **1977**, *55*, 3429−41.
(31) Green, J. L.; Lacey, A. R.; Sceats, M. G. *Chem. Phys. Lett.* **1986**, *130*, 67−71.
(32) Jeffrey, G. A. *An Introduction to Hydrogen Bonding*; Oxford University Press: New York, 1997.
(33) Michael, D.; Benjamin, I. *J. Phys. Chem.* **1995**, *99*, 1530.
(34) Devlin, J. P. *J. Chem. Phys.* **1989**, *90*, 1322−29.
(35) Kint, S.; Scherer, J. R. *J. Chem. Phys.* **1978**, *69*, 1429−31.
(36) Murphy, W. F.; Bernstein, H. J. *J. Phys. Chem.* **1972**, *76*, 1147−52.
(37) Savatinova, I.; Anachkova, E.; Nikolaeva, R. *Spectroc. Lett.* **1986**, *19*, 167−78.
(38) Wall, T. T.; Horning, D. F. *J. Chem. Phys.* **1965**, *43*, 2079−87.
(39) Wojcik, M. J.; Buch, V.; Devlin, J. P. *J. Chem. Phys.* **1993**, *99*, 2332−44.
(40) Green, J. L.; Lacey, A. R.; Sceats, M. G. *J. Phys. Chem.* **1986**, *90*, 3958−64.
(41) Sceats, M. G.; Stavola, M.; Rice, S. A. *J. Chem. Phys.* **1979**, *71*, 983−90.